Spin Symmetry Criteria for Odd-parity Magnets

Xun-Jiang Luo, ¹ Jin-Xin Hu, ¹ and K. T. Law^{1,*}

¹Department of Physics, Hong Kong University of Science and Technology, Clear Water Bay, 999077 Hong Kong, China

Inspired by the discovery of altermagnets, which exhibit even-parity nonrelativistic spin splitting, odd-parity magnets (OPMs) have been proposed and emerged as a novel research frontier. In this study, we perform a comprehensive spin group symmetry analysis to establish symmetry criteria for the emergence of OPMs. We identify eight distinct symmetry-driven cases that support OPMs, enabling their realization in collinear, coplanar, and noncoplanar magnetic orders. These OPMs are categorized into three types based on their spin textures for Bloch states: collinear (type-I), coplanar (type-II), and noncoplanar (type-III). For type-I OPMs, we further delineate additional symmetry requirements for p-wave and f-wave spin splitting. We identify 48 candidate materials in the Magndata database that satisfy these symmetry criteria. Additionally, we construct two theoretical models to validate the effectiveness of the established symmetry criteria. Finally, we show that OPMs can exhibit an intrinsic \mathbb{Z}_2 topology and construct a theoretical model to realize this phase.

Introduction.—In recent years, unconventional magnets have attracted widespread interest in condensed matter physics [1–21]. These magnets feature compensated magnetization and nonrelativistic spin splitting (NSP), where spin splitting persists in the absence of spin-orbit coupling [22–25]. This distinctive interplay of properties renders them highly promising for spintronics applications [26–31]. Among these unconventional magnets, altermagnetism is a prominent class, which acts as a third category of collinear magnetic orders in addition to ferromagnetism and antiferromagnetism [9, 11]. Altermagnets are characterized by the time-reversal symmetry breaking and alternating spin-splitting band structures with even-parity, such as d-wave or q-wave forms. Recently, odd-parity magnets (OPMs), such as p-wave, have been proposed in systems with coplanar magnetic order, broken inversion symmetry, and preserved $T\tau$ symmetry, where T is the time-reversal operation and τ represents a fractional translation [32]. Experimentally, odd-parity NSP has been confirmed in type II multiferroic material NiI_2 using photocurrent measurements [33].

The spin space group offers a comprehensive symmetry framework for systems where spin-orbit coupling is negligible [34–37], allowing the decoupling of spin and spatial degrees of freedom. This framework has proven instrumental in classifying unconventional magnets [9, 11, 38]. In particular, the spin group description of altermagnets offers a systematic guide for their prediction [9, 11], design [39-42], and manipulation [43-46] on various material platforms. In contrast, the symmetry criteria that govern OPMs remain systematically underexplored within the spin space group framework, despite preliminary proposals for their realization [32, 47, 48]. This gap presents a compelling opportunity for theoretical and experimental advancements. Furthermore, while altermagnets preclude topological insulator states (\mathbb{Z} or \mathbb{Z}_2 classification) due to time-reversal symmetry breaking and band degeneracy along high-symmetry surfaces [9, 11], OPMs can be topologically nontrivial as the existence of

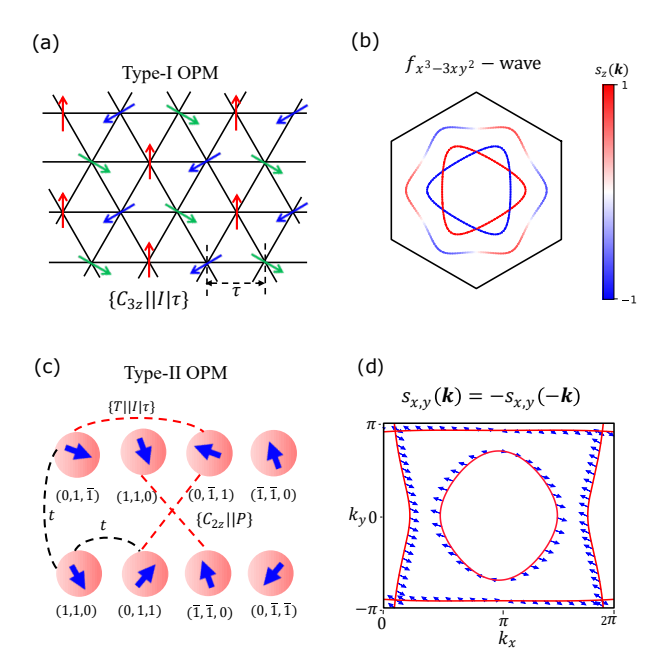


FIG. 1. (a) Schematic illustration of the 120° antiferromagnetic state on a triangle lattice with the $\sqrt{3} \times \sqrt{3}$ structures. (b) The isoenergy-surface characterized by $s_z(\mathbf{k})$ for the model shown in (a). (c) Unit cell for a 2D lattice model on a square lattice. The vectors (x, y, z) denotes the magnetic moment directions. (d) The isoenergy-surface characterized by the vector $(s_x(\mathbf{k}, s_y(\mathbf{k}))$, shown by the blue arrow, for the lattice model in (c). We take t = J = 1. In (d), $\mu = -3.2$.

effective time-reversal symmetry, allowing for a \mathbb{Z}_2 classification. The topological properties of OPMs have yet to be investigated.

In this work, we present a comprehensive symmetry analysis within the spin space group framework, establishing general symmetry criteria for the emergence of OPMs. In collinear magnetic orders, OPMs can be realized by breaking the C_2T symmetry (with C_2 being spin flipping) in conventional antiferromagnets with spin degeneracy [48]. For coplanar and noncoplanar magnetic

TABLE I. Classification of OPMs and symmetry criteria for their emergence. Column 3 details the spin texture configurations for types I-III OPMs. Columns 4 and 5 specify the symmetry criteria and corresponding magnetic orders for OPMs, respectively. Columns 6 and 7 outline additional symmetry requirements for p-wave and f-wave magnets. Here, A represents spatial operations that preserve momentum, while B denotes those that reverse momentum.

	types	spin textures	symmetries conditions	magnetic orders	p-wave	f-wave
odd- parity magnets	type-I	$s_z(oldsymbol{k}) = -s_z(-oldsymbol{k})$ $s_{x,y}(oldsymbol{k}) = 0$	$\{C_2 B\}$ and $\nexists\{C_2T A\}$	collinear		
			$\{T A au\}$ and $ mid \{C_2T A\}$	collinear	$egin{array}{ c c c c c } \{C_2 M_x\} & \{C_2 R_6\} \ p_y & f_{xyz} ext{-wa} \ \{C_2 M_y\} & \{C_2 M_{x,y}\} \ \end{array}$	$\begin{cases} f_{x^3 - 3xy^2}\text{-wave} \\ \{C_2 R_{6z} \} \end{cases}$
			(i) $\{C_z(\theta) A \tau\}$ and $\{T A \tau\}$	noncoplanar		f_{xyz} -wave
			(ii) $\{C_z(\theta) A \tau\}$ and $\{C_x(\pi) B\}$	noncoplanar		
			(iii) $\{C_z(\theta) A \tau\}$ and $\{TC_z(\pi) A\}$	coplanar	$ p_z \\ \{C_2 M_z \} $	$\begin{cases} f_{(x^2 - y^2)z} \\ \{C_2 R_{4z}, M_z\} \end{cases}$
			(iv) $\{T A \tau\}$ and $\{TC_z(\pi) A\}$	coplanar		
	type-II	$s_{x,y}(\mathbf{k}) = -s_{x,y}(-\mathbf{k})$ $s_z(\mathbf{k}) = 0$	$\{T A \tau\}$ and $\{C_z(\pi) B\}$	noncoplanar	odd-parity	
	type-III	$s_{x,y,z}(\mathbf{k}) = -s_{x,y,z}(-\mathbf{k})$	$\{T A au\}$	noncoplanar	ode	d-parity

orders, we identify six distinct symmetry-driven scenarios for OPMs [Table I]. These symmetries categorize OPMs into collinear (type-I), coplanar (type-II), and noncoplanar (type-III) spin textures for Bloch states. For type-I OPMs, we further specify additional symmetry requirements for $p_{x,y,z}$ -, $f_{x^3-3xy^2}$ -, f_{xyz} -, and $f_{(x^2-y^2)z}$ -wave NSP. Moreover, we identify 48 candidate materials in the Magndata database for OPMs and construct two theoretical models to validate the established symmetry criteria. Finally, we explore the band topology and NSP characteristics of topological OPMs in a bilayer breathing kagome lattice with nonconplanar magnetic order.

Symmetry analysis and criteria for OPMs.— We begin by discussing the spin group symmetry constraints on the spin expectation value, defined as S(k) = $(s_x(\mathbf{k}), s_y(\mathbf{k}), s_z(\mathbf{k}))$, where $s_i(\mathbf{k}) = \langle \psi_{\mathbf{k}} | \sigma_i | \psi_{\mathbf{k}} \rangle$ for i =x, y, z. Here, $\sigma_{x,y,z}$ represent the Pauli matrices in spin space, and $|\psi_{\mathbf{k}}\rangle$ denotes the Bloch state at momentum \mathbf{k} . To analyze these constraints, we introduce a spin-space group operation $g = \{X_g U_g || R_g | \tau_g\}$, where $\{R_g | \tau_g\}$ acts on the spatial coordinates (with R_g as a point group element and τ_g a fractional translation), and $\{X_gU_g\}$ operates on the spin degrees of freedom. Here, X_g is either the identity operator I or the time-reversal operator T, $U_q \in SU(2)$ is a spin rotation that can be represented by a SO(3) operation. Under the action of g, the momentum k transforms as $k \to s_q R_q k$, where $s_q = +1$ (-1) corresponds to $X_g = I(T)$. Meanwhile, the spin operator σ transforms according to $s_q U_q$. Consequently, the spin expectation value S(k) satisfies the symmetry constraint [36, 37]

$$S(s_q R_q \mathbf{k}) = s_q U_q S(\mathbf{k}). \tag{1}$$

Since the fractional translation τ_g does not contribute to the constraints on S(k), we take $\tau_g = 0$ unless otherwise stated.

There are two types of symmetries, denoted by type-a and type-b, respectively, which together fully determine the emergence of OPMs. The type a symmetries correspond to $s_g R_g \mathbf{k} = \mathbf{k}$ and $s_g U_g \neq I$, which restrict some components of $\mathbf{S}(\mathbf{k})$ to zero. The type-b symmetries correspond to $s_g R_g \mathbf{k} = -\mathbf{k}$ and $s_g U_g \neq I$, which generate the constraints on $\mathbf{S}(\mathbf{k})$ and $\mathbf{S}(-\mathbf{k})$ with excluding the inversion (P) symmetry. The type-a symmetries include spin rotation combined with translation and space-time inversion with spin rotation, represented by:

$$g_1 = \{U_q || A | \tau_q \}, \quad g_2 = \{TU_q || B \},$$
 (2)

where A preserves momentum $(A\mathbf{k} = \mathbf{k})$ and B reverses momentum $(B\mathbf{k} = -\mathbf{k})$. In three-dimensional (3D) systems, A = I and B = P are standard choices. In 2D systems, possible selections include A = I or M_z (reflection in the z-plane), and B = P, R_{2z} (a π rotation around the z-axis), PM_z , or $R_{2z}M_z$. The type-b symmetries include time-reversal combined with translation, space-inversion paired with spin rotation, and time-reversal coupled with spin rotation, expressed as:

$$g_3 = \{T | |A|\tau_q\}, \quad g_4 = \{U_q | |B\}, \quad g_5 = \{TU_q | |A\}.$$
 (3)

In the following, we derive the symmetry criteria for OPMs according to the constraints generated by g_{1-5} .

The symmetry constraints imposed by g_{1-5} can be derived using the transformation rule in Eq. (1) and depend on the specific form of U_g . Considering the compatibility of odd-parity NSP [49], without loss of generality, we

() , () , (·	
		(i)	$\mathrm{Sr_{2}Fe_{3}Se_{2}O_{3}}$
odd-	type-I	(iii)	$CsFeCl_3,\ ThMn_2,\ EuIn_2As_2,\ CsMnBr_3,\ RbFeCl_3,\ RbNiCl_3,\ CsNiCl_3,\ Ba_3CoSb_2O_9,\ CsFe(MoO_4)_2$
parity		(iv)	$\begin{array}{c} Gd_{2}BaCuO_{5},Er_{2}Pt,DyBe_{13},TbBe_{13},TbC_{2},Ca_{2}Cr_{2}O_{5},NiPS_{3},Tm_{5}Pt_{2}In_{4},\\ La_{1/3}Ca_{2/3}MnO_{3},KFe(PO_{3}F)_{2},NiCr_{2}O_{4},PrMn_{2}O_{5},HoAuGe,GdMn_{2}O_{5},\\ NaNdFeWO_{6},Sr_{2}FeO_{3}Cl,YBaFe_{4}O_{7},CeAuAl_{3},CoNb_{2}O_{6},CeNiAsO,La_{5/3}Ca_{5/8},MnO_{3},DyMn_{2}O_{5} \end{array}$
magnets	type-II		$\mathrm{Ce_{3}NIn}$
	type-III		MgV ₂ O ₄ , Mn ₅ Si ₃ , CaCoSO, BiMn ₂ O ₅ , DyFe ₃ (BO ₃) ₄ , HoFe ₃ (BO ₃) ₄ , PrFe ₃ (BO ₃) ₄ , Ba(TiO)Cu ₄ (PO ₄) ₄ , Dy ₂ Co ₃ Al ₉ , DyFeWO ₆ , Ho ₂ Cu ₂ O, BaFe ₂ Se ₃ , HoNiO ₃ , TbSbTe

TABLE II. Candidate materials for the type-I, type-II, and type-III OPMs. In type-I OPMs, the candidate materials in cases (i), (iii), (iv) satisfy the symmetry criteria associated with cases (i), (iii), (iv) in Table I.

take $U_g = C_z(\theta)$ (arbitrary rotation around z-axis) for g_1 , $U_g = C_z(\pi)$ for operations g_2 and g_5 , and $U_g = C_x(\pi)$ for g_4 . With these options, the symmetries g_{1-5} , respectively, generate the constraints

$$S(\mathbf{k}) = (0, 0, s_z(\mathbf{k})),$$

$$S(\mathbf{k}) = (s_x(\mathbf{k}), s_y(\mathbf{k}), 0),$$

$$S(\mathbf{k}) = (-s_x(-\mathbf{k}), -s_y(-\mathbf{k}), -s_z(-\mathbf{k})),$$

$$S(\mathbf{k}) = (s_x(-\mathbf{k}), -s_y(-\mathbf{k}), -s_z(-\mathbf{k})),$$

$$S(\mathbf{k}) = (s_x(-\mathbf{k}), s_y(-\mathbf{k}), -s_z(-\mathbf{k})).$$
(4)

These constraints have different effects on the components of $S(\mathbf{k})$. The symmetries g_1 and g_2 constrain two and one components of $S(\mathbf{k})$ to be zero, respectively. In contrast, the symmetries g_3 , g_4 , and g_5 flip three, two, and one components of $S(\mathbf{k})$, respectively, under the inversion of \mathbf{k} . By combining these constraints, we classify OPMs into three types based on the dimensionality d_s of the symmetry-allowed span of $S(\mathbf{k})$ in momentum space:

type-I
$$(d_s = 1)$$
: $s_i(\mathbf{k}) = -s_i(-\mathbf{k}), s_{j,l}(\mathbf{k}) = 0;$
type-II $(d_s = 2)$: $s_{i,j}(\mathbf{k}) = -s_{i,j}(-\mathbf{k}), s_l(\mathbf{k}) = 0;$
type-III $(d_s = 3)$: $s_{i,j,l}(\mathbf{k}) = -s_{i,j,l}(-\mathbf{k}),$ (5)

where $i, j, l \in \{x, y, z\}$ and $i \neq j \neq l$. The type-I OPMs, characterized by a collinear spin texture, can be realized through four kinds of combinations of symmetry operations: (i) g_1 and g_3 ; (ii) g_1 and g_4 ; (iii) g_1 and g_5 , and (iv) g_3 and g_5 [49]. In cases (i-iii), the g_1 symmetry constrains the spin textures along the z-direction and $g_{3,4,5}$ symmetries filp the z-direction spin, acting as an effective time-reversal symmetry. Case (iv) corresponds to the initial proposal for the realization of p-wave magnets [32], which belongs to case (iii) when taking $\theta = \pi$ in g_1 [49]. The type-II OPMs, exhibiting a coplanar spin texture, can be achieved by the combinations of g_3 and g_4 symmetries. Type-III OPMs are realized in systems with noncoplanar magnetic orders under the g_3 symmetry alone.

For collinear magnetic orders (with magnetization along the z direction), both g_1 and g_5 symmetries are

preserved. Under these symmetries, early studies showed that only even-parity NSP is allowed, giving rise to altermagnets [9, 11]. However, the g_5 symmetry can be broken by non-magnetic-order atoms (see Supplementary Material [49]). In such cases, OPMs can be realized in collinear antiferromagnetic systems where spin-opposite sublattices are related by inversion or translation symmetry, thereby preserving the effective time-reversal symmetry $\tilde{T} = \{C_2 || P\}$ (g_4) or $\tilde{T} = \{T || I || \tau\}$ (g_3) . This scenario has recently been investigated in several works [48, 50-55]. For coplanar magnetic orders, the q_5 symmetry is preserved and type-I OPM is realized when either g_1 or g_3 symmetry is additionally preserved. The spin textures, symmetry criteria, and magnetic orders (collinear, coplanar, or noncoplanar) for OPMs, are summarized in columns 3-5 of Table I.

In addition to preserving or reversing momentum symmetries, other spin group symmetries can also generate constraints on $S(\mathbf{k})$. For example, symmetry $g = \{C_2|R_{6z}\}$, where R_{6z} denotes a six-fold rotation around the z-axis, enforces $s_z(R_{6z}\mathbf{k}) = -s_z(\mathbf{k})$. This constraint leads to the emergence of f-wave NSP in type-I OPMs [Fig. 1(b)]. Furthermore, mirror symmetry with a π -rotation in spin space, expressed by $g_M = \{C_i(\pi)||M_j\}$, can generate the constraint

$$s_i(\mathbf{k}) = s_i(g_M \mathbf{k}), \quad s_{i,l}(\mathbf{k}) = -s_{a,l}(g_M \mathbf{k}), \tag{6}$$

where $g_M \mathbf{k} = (k_i, -k_j, k_l)$ and $i, j, l \in \{x, y, z\}$. These mirror symmetries and rotational symmetry or their combinations can lead to $p_{x,y,z}$ -wave, $f_{x^3-3xy^2}$, f_{xyz} , and $f_{(x^2-y^2)z}$ NSP in type-I OPMs, as summarized in column 6 of Table I.

Candidate materials and theoretical models for OPMs.— Using the online program FINDSPINGROUP from Ref. [35] and the Bilbao Crystallographic Server, we identify 48 candidate materials for OPMs that satisfy the established symmetry criteria, as listed in Table II. In the supplemental material [49], we identify the spin splitting patterns (p-wave or f-wave) for each candidate materials. To validate the symmetry criteria, we construct two theoretical models, H_1 and H_2 , representing type-I and

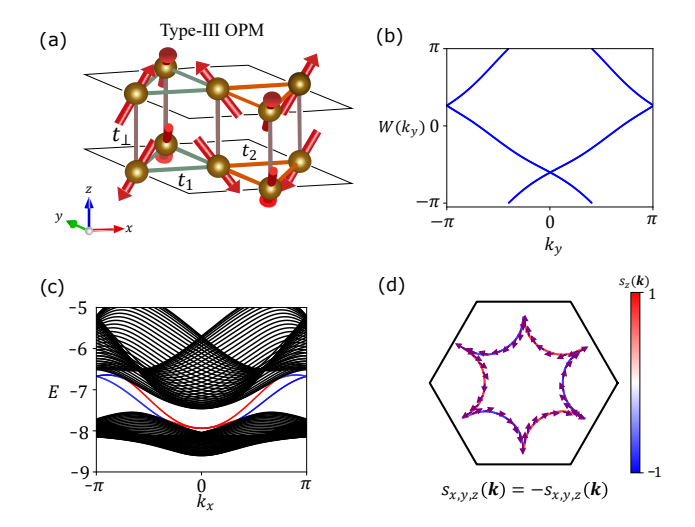


FIG. 2. (a) Schematic illustration of a bilayer kagome breathing lattice. (b) The wannier center $W(k_y)$ for the lowest energies two bands as a function of k_y . (c) The energy spectrum for the system with a nanowire geometry along the x direction. The red and blue bands denote the edge states from opposite edges. (d) The spin polarization Fermi contour. The color encodes the value $s_z(\mathbf{k})$. The pink arrows denote the direction of the vector $(s_x(\mathbf{k}), s_y(\mathbf{k}))$ at \mathbf{k} . In (b-d), $t_{\perp} = t_1 = 1$ and $t_2 = J = 4$. In (d) we take $\mu = -3.3$

type-II OPMs with coplanar [Fig. 1(a)] and noncoplanar [Fig. 1(c)] magnetic orders, respectively. The Hamiltonians H_1 and H_2 are expressed as:

$$H_{1,2} = \sum_{\langle ij \rangle} t c_{i\sigma}^{\dagger} c_{j\sigma} + J \sum_{i} \boldsymbol{m}_{i} \cdot c_{i\sigma}^{\dagger} \boldsymbol{\sigma}_{\sigma\sigma'} c_{i\sigma'},$$

where $c_{i\sigma}^{\dagger}$ ($c_{i\sigma}$) denotes the creation (annihilation) operator for an electron with spin $\sigma = \uparrow, \downarrow$ at site i, and $\langle ij \rangle$ represents summation over nearest-neighbor sites with hopping amplitude t. The second term describes the onsite exchange interaction, with strength J, between conduction electrons and localized magnetic moments m_i . The model H_1 describes a coplanar 120° antiferromagnetic state on a triangular lattice with a $\sqrt{3} \times \sqrt{3}$ structure [Fig. 1(a)], which hosts three magnetic sublattices (A, B, and C) with moments $m_A = (-\sqrt{3}/2, -1/2, 0),$ $m_{\rm B} = (\sqrt{3}/2, -1/2, 0)$, and $m_{\rm C} = (0, 1, 0)$. This model captures the g_1 and g_5 symmetries of type-I OPMs in case (iii) (Table II), with $g_1 = \{C_z(2\pi/3)|I|\tau\}$. Additionally, H_1 respects the symmetry $g_r = \{I | |R_{3z}\}$. These symmetries enforce constraints such that $s_z(\mathbf{k}) = -s_z(-\mathbf{k}) =$ $s_z(R_{3z}\mathbf{k})$, leading to $s_z(R_{6z}\mathbf{k}) = -s_z(\mathbf{k})$. This results in an f-wave NSP of the form $(k_x^3 - 3k_x k_y^2)\sigma_z$ [25], as shown in Fig. 1(b). The model H_2 is defined on a square lattice with eight magnetic sublattices, with moments illustrated in Fig. 1(c). H_2 respects symmetries $g_3 = \{T | |I|\tau\}$ and $g_4 = \{C_z(\pi)||P\}$, enabling type-II OPMs with spin textures characterized by $s_{x,y}(\mathbf{k}) = -s_{x,y}(-\mathbf{k})$, as depicted in Fig. 1(d).

Topological odd-parity magnets.— Although the magnetic orders in OPMs break the T symmetry, the system can preserve an effective time-reversal symmetry \tilde{T} satisfying $\tilde{T}^2 = -1$. This anti-unitary symmetry enables a nontrivial \mathbb{Z}_2 topological classification [56]. We demonstrate this topological phase in a bilayer breathing Kagome lattice [Fig. 2(a)], which also exhibits type-III OPM characteristics. The model Hamiltonian is given by:

$$\mathcal{H} = \sum_{\alpha\beta\sigma\ell} (t_1 \sum_{\langle ij \rangle} c^{\dagger}_{i\alpha\sigma\ell} c_{j\beta\sigma\ell} + t_2 \sum_{\langle \bar{i}j \rangle} c^{\dagger}_{i\alpha\sigma\ell} c_{j\beta\sigma\ell}) + \sum_{i\alpha\sigma\ell\ell'} t_{\perp} c^{\dagger}_{i\alpha\sigma\ell} c_{i\alpha\sigma\ell'} + \sum_{i\alpha\sigma\ell} J \boldsymbol{m}_{\alpha\ell} \cdot c^{\dagger}_{i\alpha\sigma\ell} \boldsymbol{\sigma} c_{i\alpha\sigma\ell},$$
(7)

where $\alpha, \beta = A$, B, C denote the three sublattices, and $\ell, \ell' = \mathfrak{b}, \mathfrak{t}$ represent the bottom and top layers, respectively. The first and second terms describe intracell and intercell hopping with amplitudes t_1 and t_2 , respectively. The third term represents interlayer hopping with amplitude t_{\perp} , and the fourth term accounts for noncoplanar magnetic orders through local magnetic moments $\boldsymbol{m}_{\alpha\ell}$. We set $\boldsymbol{m}_{\alpha\mathfrak{b}} = -\boldsymbol{m}_{\alpha\mathfrak{t}}$, with $\boldsymbol{m}_{A\mathfrak{t}} = (1/4, \sqrt{3}/4, \sqrt{3}/2)$, $\boldsymbol{m}_{B\mathfrak{t}} = (-1/4, \sqrt{3}/4, \sqrt{3}/2)$, and $\boldsymbol{m}_{C\mathfrak{t}} = (0, 1/2, \sqrt{3}/2)$.

The magnetic structure of a single-layer kagome lattice exhibits nonzero spin chirality, defined as $\chi = m_A \cdot (m_B \times$ $m_{\rm C}$), which can induce a Chern band topology [57]. In a bilayer kagome system, the layer-contrasted magnetic moments in \mathcal{H} preserve the symmetry $\tilde{T} = \{T | |M_z\},$ which simultaneously inverts the Chern number and layer. This symmetry enables the emergence of quantum spin Hall states protected by the T symmetry, as recently studied in Ref. [37]. In the breathing kagome lattice, the inversion symmetry is broken due to $t_1 \neq t_2$. This leads to nondegenerate bulk bands, exhibiting odd-parity spin splitting. Consequently, \mathcal{H} describes a topological OPM. A standard Wilson loop calculation [58] for the lowest two bulk bands, shown in Fig. 2(b), confirms their nontrivial \mathbb{Z}_2 topology. Fig. 2(c) illustrates the helical edge states in a nanowire geometry. Fig. 2(d) depicts isoenergy Fermi surfaces with odd-parity spin polarization. The numerical results further reveal that the spin texture satisfies $S(R_{3z}\mathbf{k}) = C_z(2\pi/3)S(\mathbf{k})$, which is consistent with the presence of symmetry $\{C_z(2\pi/3)||R_{3z}\}.$

Discussion and summary.— Altermagnets, characterized by their alternating NSP with even-parity in collinear magnetic orders, have been extensively studied. We emphasize that our framework also allows for a systematic exploration of even-parity NSP, beyond collinear magnets. For instance, combining symmetries g_1 and g_5 with the choice of $U_g = C_x(\pi)$ for g_5 results in $s_z(\mathbf{k}) = s_z(-\mathbf{k})$ and $s_{x,y}(\mathbf{k}) = 0$. Furthermore, specific symmetry, such as g_5 along, can lead to hybrid-parity behaviors, where NSP exhibits even-parity for $s_{x,y}(\mathbf{k})$, and odd-parity for $s_z(\mathbf{k})$, which can give rise to spin current [26] and Edelstein effect [59], respectively. These phenomena are crucial for read and write operations in

spintronics [60]. We systematically explore the symmetry criteria for these cases in our future work.

In OPMs, time-reversal symmetry T is explicitly broken. However, effective time-reversal symmetries, such as $\{T||\tau\}$ and $\{TC_z(\pi)||I\}$, can be preserved, leading to odd-parity spin textures. These textures are effectively described by nonrelativistic spin-orbit coupling and are compatible with s-wave superconducting pairing [61, 62]. Notably, these effective symmetries do not enforce Kramers degeneracy at all time-reversal invariant momenta [63], resulting in a significant magnetic energy gap at these points. Consequently, the band structures of OPMs are shaped by the interplay of effective spin-orbit coupling and Zeeman fields, as best exemplified in 1D helimagnets [64]. These unique band structures position OPMs as ideal materials for investigating topological superconductors [64], which will be explored in our future study.

In summary, through a comprehensive symmetry analysis within the spin space group framework, we establish general criteria for the emergence of OPMs and identify 47 candidate materials. Our work advances the theoretical understanding of OPMs and provides a foundation for future experimental and theoretical investigations.

ACKNOWLEDGMENT

We acknowledge useful discussions with Junwei Liu, Xin Liu, Fengcheng Wu, and Xilin Feng. K.T.L acknowledges the support from the Ministry of Science and Technology, China, and Hong Kong Research Grant Council through Grants No. 2020YFA0309600, No. RFS2021-6S03, No. C6025-19G, No. AoE/P-701/20, No. 16310520, No. 16307622, and No. 16309223.

- * phlaw@ust.hk
- H. Chen, Q. Niu, and A. H. MacDonald, Anomalous hall effect arising from noncollinear antiferromagnetism, Phys. Rev. Lett. 112, 017205 (2014).
- [2] S. Nakatsuji, N. Kiyohara, and T. Higo, Large anomalous hall effect in a non-collinear antiferromagnet at room temperature, Nature 527, 212 (2015).
- [3] J. Zelezný, Y. Zhang, C. Felser, and B. Yan, Spin-polarized current in noncollinear antiferromagnets, Phys. Rev. Lett. 119, 187204 (2017).
- [4] Y. Zhang, Y. Sun, H. Yang, J. Zelezný, S. P. P. Parkin, C. Felser, and B. Yan, Strong anisotropic anomalous hall effect and spin hall effect in the chiral antiferromagnetic compounds mn_3x (x = Ge, sn, ga, ir, rh, and pt), Phys. Rev. B **95**, 075128 (2017).
- [5] L. Smejkal, Y. Mokrousov, B. Yan, and A. H. Mac-Donald, Topological antiferromagnetic spintronics, Nature Physics 14, 242 (2018).
- [6] L. Smejkal, R. González-Hernández, T. Jungwirth, and J. Sinova, Crystal time-reversal symmetry breaking and

- spontaneous hall effect in collinear antiferromagnets, Science Advances 6, eaaz8809 (2020).
- [7] H.-Y. Ma, M. Hu, N. Li, J. Liu, W. Yao, J.-F. Jia, and J. Liu, Multifunctional antiferromagnetic materials with giant piezomagnetism and noncollinear spin current, Nature Communications 12, 2846 (2021).
- [8] Z. Feng, X. Zhou, L. Smejkal, L. Wu, Z. Zhu, H. Guo, R. González-Hernández, X. Wang, H. Yan, P. Qin, X. Zhang, H. Wu, H. Chen, Z. Meng, L. Liu, Z. Xia, J. Sinova, T. Jungwirth, and Z. Liu, An anomalous hall effect in altermagnetic ruthenium dioxide, Nature Electronics 5, 735 (2022).
- [9] L. Smejkal, J. Sinova, and T. Jungwirth, Emerging research landscape of altermagnetism, Phys. Rev. X 12, 040501 (2022).
- [10] L. Smejkal, A. B. Hellenes, R. González-Hernández, J. Sinova, and T. Jungwirth, Giant and tunneling magnetoresistance in unconventional collinear antiferromagnets with nonrelativistic spin-momentum coupling, Phys. Rev. X 12, 011028 (2022).
- [11] L. Smejkal, J. Sinova, and T. Jungwirth, Beyond conventional ferromagnetism and antiferromagnetism: A phase with nonrelativistic spin and crystal rotation symmetry, Phys. Rev. X 12, 031042 (2022).
- [12] H. Bai, Y. C. Zhang, Y. J. Zhou, P. Chen, C. H. Wan, L. Han, W. X. Zhu, S. X. Liang, Y. C. Su, X. F. Han, F. Pan, and C. Song, Efficient spin-to-charge conversion via altermagnetic spin splitting effect in antiferromagnet ruo₂, Phys. Rev. Lett. 130, 216701 (2023).
- [13] J. Krempaský, L. Smejkal, S. W. D'Souza, M. Hajlaoui, G. Springholz, K. Uhlírová, F. Alarab, P. C. Constantinou, V. Strocov, D. Usanov, W. R. Pudelko, R. González-Hernández, A. Birk Hellenes, Z. Jansa, H. Reichlová, Z. Sobán, R. D. Gonzalez Betancourt, P. Wadley, J. Sinova, D. Kriegner, J. Minár, J. H. Dil, and T. Jungwirth, Altermagnetic lifting of kramers spin degeneracy, Nature 626, 517 (2024).
- [14] X. Zhou, W. Feng, R.-W. Zhang, L. Smejkal, J. Sinova, Y. Mokrousov, and Y. Yao, Crystal thermal transport in altermagnetic ruo₂, Phys. Rev. Lett. 132, 056701 (2024).
- [15] S. Reimers, L. Odenbreit, L. Smejkal, V. N. Strocov, P. Constantinou, A. B. Hellenes, R. Jaeschke Ubiergo, W. H. Campos, V. K. Bharadwaj, A. Chakraborty, T. Denneulin, W. Shi, R. E. Dunin-Borkowski, S. Das, M. Kläui, J. Sinova, and M. Jourdan, Direct observation of altermagnetic band splitting in crsb thin films, Nature Communications 15, 2116 (2024).
- [16] L. Bai, W. Feng, S. Liu, L. Smejkal, Y. Mokrousov, and Y. Yao, Altermagnetism: Exploring new frontiers in magnetism and spintronics, Advanced Functional Materials 34, 2409327 (2024).
- [17] P. A. McClarty and J. G. Rau, Landau theory of altermagnetism, Phys. Rev. Lett. 132, 176702 (2024).
- [18] S. Lee, S. Lee, S. Jung, J. Jung, D. Kim, Y. Lee, B. Seok, J. Kim, B. G. Park, L. Smejkal, C.-J. Kang, and C. Kim, Broken kramers degeneracy in altermagnetic mnte, Phys. Rev. Lett. 132, 036702 (2024).
- [19] X. Chen, Y. Liu, P. Liu, Y. Yu, J. Ren, J. Li, A. Zhang, and Q. Liu, Unconventional magnons in collinear magnets dictated by spin space groups, Nature 640, 349 (2025).
- [20] M. Hu, X. Cheng, Z. Huang, and J. Liu, Catalog of c-paired spin-momentum locking in antiferromagnetic systems, Phys. Rev. X 15, 021083 (2025).

- [21] H. Zhu, J. Li, X. Chen, Y. Yu, and Q. Liu, Magnetic geometry induced quantum geometry and nonlinear transports, Nature Communications 16, 4882 (2025).
- [22] M. Naka, S. Hayami, H. Kusunose, Y. Yanagi, Y. Motome, and H. Seo, Spin current generation in organic antiferromagnets, Nature Communications 10, 4305 (2019).
- [23] S. Hayami, Y. Yanagi, and H. Kusunose, Momentum-dependent spin splitting by collinear antiferromagnetic ordering, Journal of the Physical Society of Japan 88, 123702 (2019).
- [24] L.-D. Yuan, Z. Wang, J.-W. Luo, E. I. Rashba, and A. Zunger, Giant momentum-dependent spin splitting in centrosymmetric low-z antiferromagnets, Phys. Rev. B 102, 014422 (2020).
- [25] S. Hayami, Y. Yanagi, and H. Kusunose, Spontaneous antisymmetric spin splitting in noncollinear antiferromagnets without spin-orbit coupling, Phys. Rev. B 101, 220403 (2020).
- [26] R. González-Hernández, L. Smejkal, K. Výborný, Y. Yahagi, J. Sinova, T. c. v. Jungwirth, and J. Zelezný, Efficient electrical spin splitter based on nonrelativistic collinear antiferromagnetism, Phys. Rev. Lett. 126, 127701 (2021).
- [27] R.-W. Zhang, C. Cui, R. Li, J. Duan, L. Li, Z.-M. Yu, and Y. Yao, Predictable gate-field control of spin in altermagnets with spin-layer coupling, Phys. Rev. Lett. 133, 056401 (2024).
- [28] L. Han, X. Fu, R. Peng, X. Cheng, J. Dai, L. Liu, Y. Li, Y. Zhang, W. Zhu, H. Bai, Y. Zhou, S. Liang, C. Chen, Q. Wang, X. Chen, L. Yang, Y. Zhang, C. Song, J. Liu, and F. Pan, Electrical 180° switching of néel vector in spin-splitting antiferromagnet, Science Advances 10, eadn0479 (2024).
- [29] Z. Zhou, X. Cheng, M. Hu, R. Chu, H. Bai, L. Han, J. Liu, F. Pan, and C. Song, Manipulation of the altermagnetic order in crsb via crystal symmetry, Nature 638, 645 (2025).
- [30] Y. Zhang, H. Bai, J. Dai, L. Han, C. Chen, S. Liang, Y. Cao, Y. Zhang, Q. Wang, W. Zhu, F. Pan, and C. Song, Electrical manipulation of spin splitting torque in altermagnetic ruo2, Nature Communications 16, 5646 (2025).
- [31] J.-X. Hu, O. Matsyshyn, and J. C. Song, Nonlinear superconducting magnetoelectric effect, Physical Review Letters 134, 026001 (2025).
- [32] A. Birk Hellenes, T. Jungwirth, R. Jaeschke-Ubiergo, A. Chakraborty, J. Sinova, and L. Smejkal, P-wave magnets, arXiv:2309.01607.
- [33] Q. Song, S. Stavrić, P. Barone, A. Droghetti, D. S. Antonenko, J. W. F. Venderbos, C. A. Occhialini, B. Ilyas, E. Ergeçen, N. Gedik, S.-W. Cheong, R. M. Fernandes, S. Picozzi, and R. Comin, Electrical switching of a p-wave magnet, Nature 642, 64 (2025).
- [34] P. Liu, J. Li, J. Han, X. Wan, and Q. Liu, Spin-group symmetry in magnetic materials with negligible spinorbit coupling, Phys. Rev. X 12, 021016 (2022).
- [35] X. Chen, J. Ren, Y. Zhu, Y. Yu, A. Zhang, P. Liu, J. Li, Y. Liu, C. Li, and Q. Liu, Enumeration and representation theory of spin space groups, Phys. Rev. X 14, 031038 (2024).
- [36] Y. Jiang, Z. Song, T. Zhu, Z. Fang, H. Weng, Z.-X. Liu, J. Yang, and C. Fang, Enumeration of spin-space groups: Toward a complete description of symmetries of magnetic orders, Phys. Rev. X 14, 031039 (2024).

- [37] Z. Xiao, J. Zhao, Y. Li, R. Shindou, and Z.-D. Song, Spin space groups: Full classification and applications, Phys. Rev. X 14, 031037 (2024).
- [38] Y. Liu, X. Chen, Y. Yu, and Q. Liu, Symmetry Classification of Magnetic Orders and Emergence of Spin-Orbit Magnetism, arXiv:2506.20739 (2025).
- [39] I. Mazin, R. González-Hernández, and L. Smejkal, Induced Monolayer Altermagnetism in MnP(S,Se)₃ and FeSe, arXiv:2309.02355 (2023).
- [40] Y. Sheng, J. Liu, J. Zhang, and M. Wu, Ubiquitous van der Waals altermagnetism with sliding/moire ferroelectricity, arXiv:2411.17493 (2024).
- [41] Y. Liu, J. Yu, and C.-C. Liu, Twisted magnetic van der waals bilayers: An ideal platform for altermagnetism, Phys. Rev. Lett. 133, 206702 (2024).
- [42] W. Sun, C. Yang, W. Wang, Y. Liu, X. Wang, S. Huang, and Z. Cheng, Proposing altermagnetic-ferroelectric type-iii multiferroics with robust magnetoelectric coupling, Advanced Materials 37, 2502575 (2025).
- [43] W. Sun, W. Wang, C. Yang, R. Hu, S. Yan, S. Huang, and Z. Cheng, Altermagnetism induced by sliding ferroelectricity via lattice symmetry-mediated magnetoelectric coupling, Nano Letters 24, 11179 (2024).
- [44] M. Gu, Y. Liu, H. Zhu, K. Yananose, X. Chen, Y. Hu, A. Stroppa, and Q. Liu, Ferroelectric switchable altermagnetism, Phys. Rev. Lett. 134, 106802 (2025).
- [45] Y. Che, H. Lv, X. Wu, and J. Yang, Engineering altermagnetic states in two-dimensional square tessellations, Phys. Rev. Lett. 135, 036701 (2025).
- [46] X. Duan, J. Zhang, Z. Zhu, Y. Liu, Z. Zhang, I. Zutić, and T. Zhou, Antiferroelectric altermagnets: Antiferroelectricity alters magnets, Phys. Rev. Lett. 134, 106801 (2025).
- [47] Y. Yu, M. B. Lyngby, T. Shishidou, M. Roig, A. Kreisel, M. Weinert, B. M. Andersen, and D. F. Agterberg, Odd-parity Magnetism Driven by Antiferromagnetic Exchange, arXiv:2501.02057 (2025).
- [48] Y.-P. Lin, Odd-parity altermagnetism through sublattice currents: From Haldane-Hubbard model to general bipartite lattices, arXiv:2503.09602 (2025).
- 49 See supplemental material.
- [50] M. Zeng, Z. Qin, L. Qin, S. Feng, D.-H. Xu, and R. Wang, The electronic and transport properties in the Haldane-Hubbard with odd-parity altermagnetism, arXiv:2507.09906 (2025).
- [51] S. Huang, Z. Qin, F. Zhan, D.-H. Xu, D.-S. Ma, and R. Wang, Light-induced Odd-parity Magnetism in Conventional Collinear Antiferromagnets, arXiv:2507.20705 (2025).
- [52] B. Li, D.-F. Shao, and A. A. Kovalev, Floquet Spin Splitting and Spin Generation in Antiferromagnets, arXiv:2507.22884 (2025).
- [53] T. Zhu, D. Zhou, H. Wang, and J. Ruan, Floquet oddparity collinear magnets, arXiv:2508.02542 (2025).
- [54] Z.-Y. Zhuang, D. Zhu, D. Liu, Z. Wu, and Z. Yan, Odd-Parity Altermagnetism Originated from Orbital Orders, arXiv:2508.18361 (2025).
- [55] D. Liu, Z.-Y. Zhuang, D. Zhu, Z. Wu, and Z. Yan, Lightinduced odd-parity altermagnets on dimerized lattices, arXiv:2508.18360 (2025).
- [56] C.-K. Chiu, J. C. Y. Teo, A. P. Schnyder, and S. Ryu, Classification of topological quantum matter with symmetries, Rev. Mod. Phys. 88, 035005 (2016).

- [57] K. Ohgushi, S. Murakami, and N. Nagaosa, Spin anisotropy and quantum hall effect in the kagomé lattice: Chiral spin state based on a ferromagnet, Phys. Rev. B 62, R6065 (2000).
- [58] R. Yu, X. L. Qi, A. Bernevig, Z. Fang, and X. Dai, Equivalent expression of F_2 topological invariant for band insulators using the non-abelian berry connection, Phys. Rev. B 84, 075119 (2011).
- [59] R. González-Hernández, P. Ritzinger, K. Výborný, J. Zelezný, and A. Manchon, Non-relativistic torque and edelstein effect in non-collinear magnets, Nature Communications 15, 7663 (2024).
- [60] A. Manchon, J. Zelezný, I. M. Miron, T. Jungwirth, J. Sinova, A. Thiaville, K. Garello, and P. Gambardella, Current-induced spin-orbit torques in ferromagnetic and

- antiferromagnetic systems, Rev. Mod. Phys. **91**, 035004 (2019).
- [61] Z.-T. Sun, X. Feng, Y.-M. Xie, B. T. Zhou, J.-X. Hu, and K. T. Law, Pseudo-Ising superconductivity induced by p-wave magnetism, arXiv:2501.10960 (2025).
- [62] P. Sukhachov, H. G. Giil, B. Brekke, and J. Linder, Coexistence of p-wave magnetism and superconductivity, Phys. Rev. B 111, L220403 (2025).
- [63] Y. B. Kudasov, Topological band structure due to modified kramers degeneracy for electrons in a helical magnetic field, Phys. Rev. B 109, L140402 (2024).
- [64] I. Martin and A. F. Morpurgo, Majorana fermions in superconducting helical magnets, Phys. Rev. B 85, 144505 (2012).